Applied Surface Science 569 (2021) 150878

Contents lists available at ScienceDirect

Applied Surface Science

journal homepage: www.elsevier.com/locate/apsusc

Full Length Article

Smoothing surface roughness using Al_2O_3 atomic layer deposition

Tyler J. Myers [a], James A. Throckmorton [b], Rebecca A. Borrelli [b], Malcolm O'Sullivan [b], Tukaram Hatwar [b], Steven M. George [a,*]

[a] Department of Chemistry, University of Colorado, Boulder, CO 80309, USA
[b] L3Harris, Space & Airborne Systems, 2696 Manitou Road, Rochester, NY 14624, USA

ARTICLE INFO

Keywords:
Surface smoothing
Surface roughness
Atomic layer deposition
Atomic force microscopy
White light interferometry
Optical reflectivity

ABSTRACT

Al_2O_3 atomic layer deposition (ALD) was used to smooth the roughness on silicon wafers obtained prior to chemical mechanical polishing (CMP). The initial silicon wafers had an average RMS surface roughness of 3.3 nm as determined by atomic force microscopy (AFM) measurements. AFM line scans also measured an average lateral spacing of ≈490 nm between the surface asperities. The RMS roughness decreased and the average lateral spacing increased progressively with number of Al_2O_3 ALD cycles. After 3000 Al_2O_3 ALD cycles that deposit an Al_2O_3 film thickness of 370 nm, the RMS roughness reduced to 1.5 nm and the average lateral spacing between the surface asperities increased to ≈890 nm. Additional Al_2O_3 ALD cycles produced little change in the RMS roughness or average lateral spacing. The efficiency of the smoothing decreased when the lateral distance between the surface asperities was much larger than the Al_2O_3 ALD film thickness. Power spectral density (PSD) analysis revealed that the ALD smoothing was most effective for surface topographical features with lateral spacings in the range of 10s to 100s of nanometers. Reflectivity studies of silver films deposited on the silicon wafers also demonstrated that Al_2O_3 ALD smoothing improved the optical performance of reflective mirrors.

1. Introduction

Surface roughness affects numerous areas including semiconductor devices[1,2], optical performance [3,4], friction [5], and adhesion [6,7]. There are many processes used to smooth surfaces including chemical etching [8], chemical mechanical polishing (CMP) [9,10], magnetorheological finishing [11], electrochemical micromachining [12], and ion beam erosion [13]. These processes can smooth efficiently, but can also change the surface curvature or damage the underlying substrate. Many surface smoothing processes would benefit from an alternative smoothing technique that removes roughness without negatively impacting the surface. This is particularly important for optical applications where smooth initial substrates with precise curvature are needed for the deposition of metals to fabricate reflective mirrors.

Atomic layer deposition (ALD) is a thin film deposition method that coats materials with atomic scale control [14]. In the ALD process, typically two gas-phase reactants are introduced sequentially to a substrate to precisely deposit the ALD material. These sequential surface reactions are self-limiting, meaning once all surface sites have reacted, the reaction effectively saturates. This growth technique allows for precise digital control of film thickness. ALD has been used to deposit various materials including numerous oxides, nitrides and sulfides [15].

Due to the self-limiting nature of the surface reactions, films deposited by ALD are highly conformal and cover the surface with a uniform layer of material. This conformality allows ALD to act as the reverse of CMP. Rather than etching away the surface asperities, ALD can "pinch-off" surface roughness by filling in the gaps between the surface features. An idealization of this procedure is illustrated in Fig. 1. Each ALD cycle deposits a conformal film on the underlying substrate. The gaps between the surface asperities are progressively filled in by the ALD film. The gaps are closed when the ALD film thickness is one-half of the distance between the surface asperities.

There have been some reports on substrate smoothing by ALD [16–20]. However, these previous studies have not precisely quantified ALD smoothing versus ALD cycles. The earlier investigations have also not explored the relationship between ALD smoothing and the lateral spacing between the surface asperities that define the surface roughness. Al_2O_3 ALD was discovered to smooth the roughness of polycrystalline tungsten and zinc oxide films in W/Al_2O_3 and ZnO/Al_2O_3 nanolaminates [17,20]. TiO_2 ALD was also shown to smooth scalloped surfaces and decreased their surface area versus TiO_2 ALD film thickness [16]. In addition, Al_2O_3 ALD on porous ceramic membranes was noticed to close

* Corresponding author.
E-mail address: steven.george@colorado.edu (S.M. George).

https://doi.org/10.1016/j.apsusc.2021.150878
Received 9 June 2021; Received in revised form 3 August 2021; Accepted 5 August 2021
Available online 13 August 2021

the pores and visibly smooth the porous membranes [19]. Al_2O_3 ALD was also observed to reduce the RMS surface roughness of polycrystalline ZnO films [18].

Surface roughness can affect optical device performance. For example, surface roughness can affect the reflectivity of mirrors by increasing scattering. Scattering occurs when light interacts with features larger than the light wavelength. When light scatters from a rough surface, some light will specularly reflect at the same angle as the incident light. Other light will be diffusely reflected at non-specular angles. The surface roughness features can be described as a superposition of sinusoidal structures that will lead to diffuse scattering resulting from diffraction [21].

Surface absorption can also affect mirror reflectivity when light interacts with features smaller than the light wavelength on some metallic surfaces. The surface absorption is most noticeable in nanostructures of metals such as silver, gold and platinum that have large plasmon resonances. On silver surfaces with nanometer scale roughness, light can easily excite surface plasmons [22,23]. These surface plasmons can then be absorbed by the silver.

Conventional techniques that can smooth substrates often negatively affect the curvature. Consequently, additional processing steps are required to correct the curvature. ALD may be able to overcome this problem and smooth the surface roughness of a substrate for reflective mirror fabrication without affecting its curvature. In addition, ALD can be scaled up to accommodate large mirror substrates. Compared with other smoothing techniques, ALD is also an additive process that can improve surface roughness without being destructive.

2. Materials and methods

2.1. Initial substrates and film deposition

Experiments were performed in a hot-walled, viscous flow reactor that has been described previously [24]. A rough, pre-CMP silicon-on-insulator (SOI) silicon wafer from Soitec was cut into 2×2 cm^2 coupons. For each coating run, one pre-CMP SOI coupon and a standard SOI coupon were cleaned with isopropanol, followed by water, and then dried under N_2. Both coupons were introduced into the reactor and heated to 200 °C on a stainless steel boat. The coupons were allowed to equilibrate in the reactor for 30 min before beginning the ALD.

Al_2O_3 ALD was performed using trimethylaluminum (TMA, 97% Sigma) and reagent-grade water (H_2O, Sigma) at 200 °C [25]. The reactor was operated in viscous flow [24]. Reactants were dosed sequentially into a N_2 carrier gas. The chamber pressure was ~ 1.1 Torr with 200 sccm of N_2 flowing through the chamber controlled by mass flow controllers (MKS). The ALD cycle consisted of a 1 s TMA dose, followed by a N_2 purge for 15 s, then a 1 s H_2O dose, followed by another 15 s N_2 purge. This reactant sequence is designated as 1–15-1–15. The Al_2O_3 ALD growth rate per cycle was 0.12 nm. Al_2O_3 ALD was performed for up to 4000 cycles. Typical reactant pressures were 140 mTorr for TMA and 90 mTorr for H_2O. The chamber was pumped using a dual stage rotary vane mechanical pump.

2.2. Film characterization and reflectance measurements

Al_2O_3 film thicknesses were measured on the silicon witness wafers using a spectroscopic ellipsometer (M−2000D, J. A. Woollam). The AFM measurements were performed using an atomic force microscope (Nanosurf EasyScan 2). The scanner was fitted with a 10 μm head and conical AFM tips (Aspire CT170R) as the probe. The AFM was operated in tapping mode and acquired 8.5 μm × 8.5 μm images at 1 line/s and 256 pixels/line. The AFM data and power spectral density (PSD) analysis was processed using Gwyddion. White light interferometry (WLI) measurements were performed using a Zygo NewView 7300 scanning white light microscope. The WLI data was analyzed using Metropro software.

The original pre-CMP silicon-on-insulator (SOI) silicon wafers and the subsequent ALD-coated wafers were then coated with a protected silver reflective surface. This coating was deposited using an E-beam physical vapor deposition (PVD) chamber at L3Harris. Reflectance measurements were then conducted using a Cary 7000 spectrophotometer with a calibrated reflectance range from 350 to 2400 nm.

3. Results and discussion

3.1. AFM measurements of surface roughness

Fig. 2a and 2b display an AFM image and a representative AFM line scan, respectively, of the original, rough silicon surface. Notice the different scales of the x and z axes on the line profile of Fig. 2b. The z-axis is in nanometers while the x-axis is in microns. The initial pre-CMP silicon surface has an RMS roughness of 3.3 nm. The RMS roughness is a measure of the vertical surface roughness. In contrast, the average lateral distance between the asperities on the surface is a measure of the lateral surface roughness. The surface asperities in Fig. 2b have a mean lateral distance of ≈490 nm. The lateral spacing of surface asperities is orders of magnitude larger than the vertical deviations.

Since ALD is a conformal process, the deposited ALD film will cover the original substrate with a uniform layer of material. Material will be added at the bottom of valleys, the tops of peaks, and on the sides of the asperities. Mechanistically, this means that roughness removal is possible when the ALD film approaches itself from the adjacent walls of surface asperities to overlap and fill in the troughs. The filling of the valleys between the surface peaks with Al_2O_3 ALD will "pinch-off" the surface roughness as illustrated in Fig. 1.

The ability of ALD to smooth the surface is dependent on the lateral distance between the surface peaks. The lateral distance between surface asperities is more important than the vertical surface RMS roughness in determining the ability of Al_2O_3 ALD to smooth the surface. For the surface in Fig. 2b, an ALD process depositing film thicknesses on the scale of the RMS roughness of 3.5 nm would show little to no smoothing effect. The ALD film thickness must be comparable with one-half the average lateral distance between the surface asperities to see significant surface smoothing. Consequently, surface smoothing for the surface in Fig. 2b will require film thicknesses on the order of 490 nm/2 = 245 nm.

Fig. 3a and 3b show an AFM image and a representative AFM line scan, respectively, of the original silicon surface after 1500 Al_2O_3 ALD

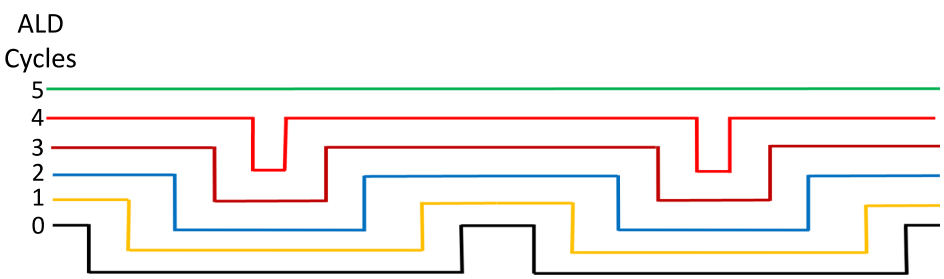

Fig. 1. Illustration of ALD on rough surface. Gaps between surface asperities are progressively "filled-in" by ALD film.

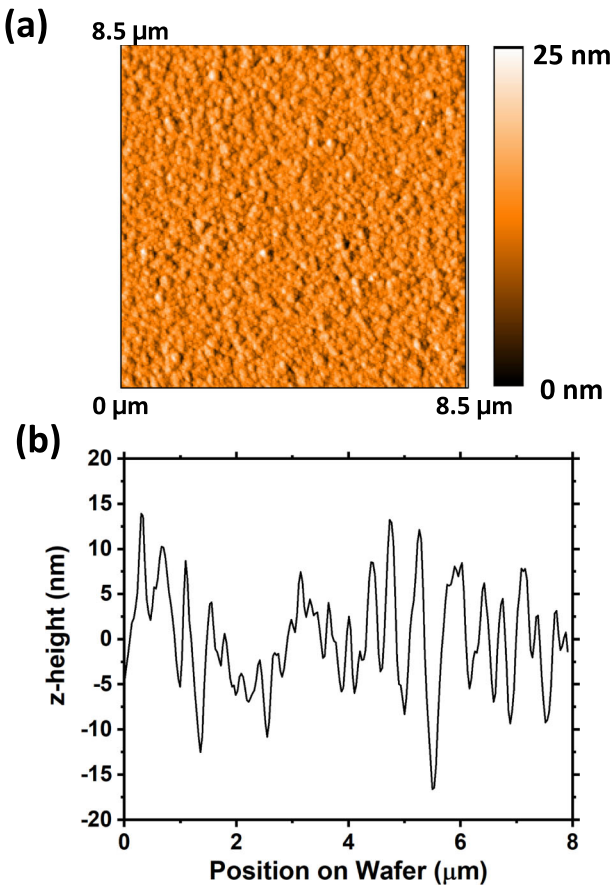

Fig. 2. (a) AFM image and (b) representative AFM line scan of rough, pre-CMP silicon wafer.

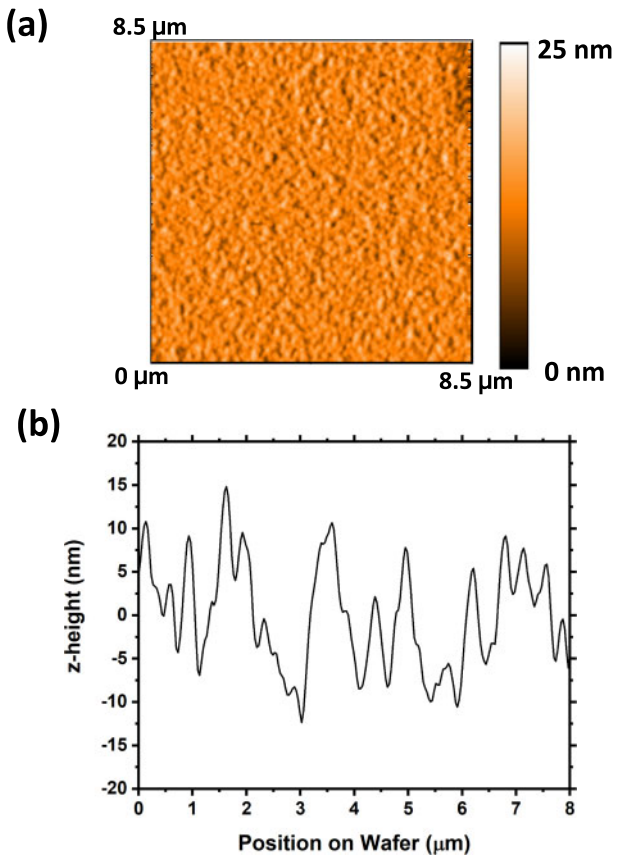

Fig. 3. (a) AFM image and (b) representative AFM line scan of rough, pre-CMP silicon wafer after 1500 Al_2O_3 ALD cycles that deposit an Al_2O_3 film thickness of 165 nm.

cycles. The 1500 Al_2O_3 ALD cycles deposited an Al_2O_3 film thickness of 165 nm as measured by spectroscopic ellipsometry. The AFM measurements in Fig. 3a revealed that the RMS surface roughness decreased from 3.3 nm to 2.0 nm. The AFM line scan after ALD plotted on the same scale as the original rough surface in Fig. 2b also shows a decrease in the height of the surface asperities in agreement with the decrease in the RMS surface roughness.

The average lateral distance between the surface asperities in Fig. 3b also increases from ≈490 nm for the original surface to ≈700 nm for the surface after 1500 Al_2O_3 ALD cycles. The increase in the lateral distance between the surface peaks is evidence of the "pinching-off" of surface asperities that are close together. Qualitatively, the sharp, tall features observed in Fig. 2b have been rounded off and have a larger separation distance following the 1500 Al_2O_3 ALD cycles.

Fig. 4a and 4b present an AFM image and a representative AFM line scan, respectively, of the original silicon surface after 3000 Al_2O_3 ALD cycles. The 3000 Al_2O_3 ALD cycles deposited an Al_2O_3 film thickness of 370 nm as measured by spectroscopic ellipsometry. The AFM measurements in Fig. 4a revealed that the RMS surface roughness decreased to 1.5 nm. Comparison with the original rough surface in Fig. 2b again reveals a further decrease in the height of the surface asperities in agreement with the decrease in the RMS surface roughness.

The average lateral distance between the surface asperities in Fig. 4b also increases from ≈490 nm for the original surface to ≈890 nm for the surface after 3000 Al_2O_3 ALD cycles. The increase in the lateral distance between the surface peaks is further evidence of the "pinching-off" of surface asperities with increasing Al_2O_3 ALD film thickness. The comparison between Fig. 2b and Fig. 4b is direct visual evidence that the Al_2O_3 ALD film thickness can smooth the surface roughness.

3.2. *RMS surface roughness and lateral distance between surface asperities*

The RMS surface roughness versus number of Al_2O_3 ALD cycles is shown in Fig. 5. The RMS surface roughness decreases approximately linearly for the first 1000 Al_2O_3 ALD cycles from the average starting RMS surface roughness of ≈3.3 nm. The change in the RMS surface roughness then begins to slow before leveling off at approximately 1.5 nm after 3000 Al_2O_3 ALD cycles. There is a small increase of < 0.1 nm in RMS roughness between 3500 and 4000 ALD cycles. This small increase may be attributed to slightly rougher initial surfaces on average for the 4000 ALD cycle experiments.

The limiting behavior of the smoothing effect in Fig. 5 is believed to be caused by the increase of the lateral distance between surface asperities as the ALD fills in the valleys between the surface peaks. The average spacing between the surface asperities is displayed in Fig. 6. The surface peaks that are the closest together will be "pinched-off" first. The average lateral distance between the surface asperities on the initial rough surface in Fig. 2b was ≈490 nm. As the valleys are filled in, the surface asperities that remain will be progressively further apart. The average lateral distance between the surface asperities increased to ≈890 nm after 3000 ALD cycles.

Eventually, the valleys between the surface peaks are too wide to be affected by the ALD film thickness. Fig. 5 reveals that the ability of the Al_2O_3 ALD film thickness to smooth the surface roughness becomes limited after $>$ 2000 ALD cycles. The 2000 ALD cycles deposit an Al_2O_3 ALD film thickness of 240 nm. Half the distance between the initial surface asperities is 490 nm/2 = 245 nm. In agreement with expectations, the smoothing effect of the Al_2O_3 ALD decreases when the thickness of the Al_2O_3 ALD film is approximately one-half the average

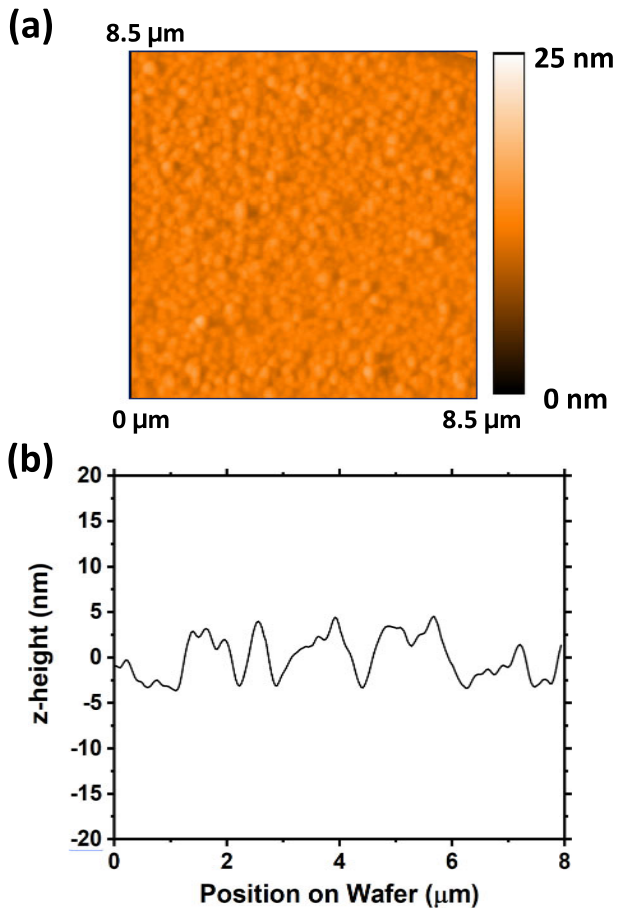

Fig. 4. (a) AFM image and (b) representative AFM line scan of rough, pre-CMP silicon wafer after 3000 Al_2O_3 ALD cycles that deposit an Al_2O_3 film thickness of 370 nm.

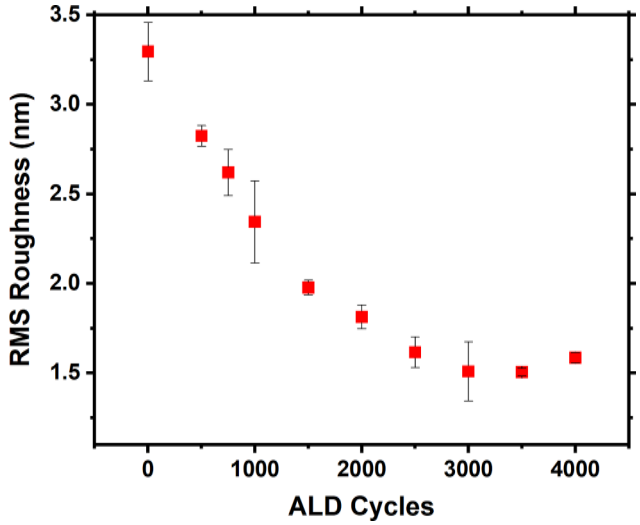

Fig. 5. RMS roughness versus number of Al_2O_3 ALD cycles on an initial rough, pre-CMP silicon wafer.

distance between the surface asperities.

The change in the RMS surface roughness versus Al_2O_3 ALD film thickness decreases progressively for thicker Al_2O_3 ALD films. Fig. 7 shows the change in the RMS roughness for every additional 500 Al_2O_3 ALD cycles. The average lateral spacing between the surface asperities is

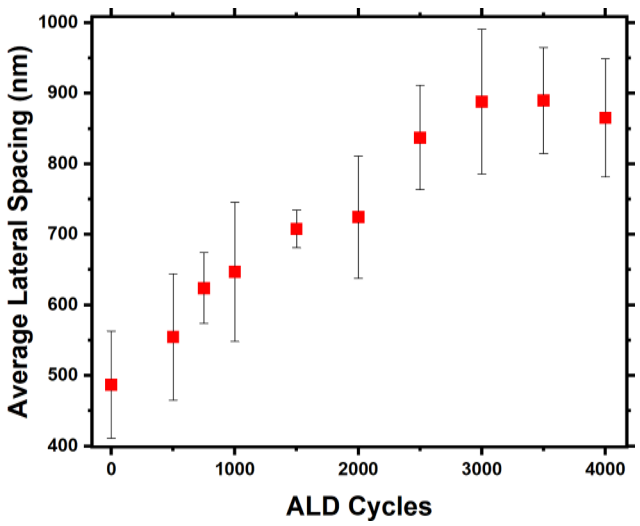

Fig. 6. Average lateral spacing between the surface asperities versus number of Al_2O_3 ALD cycles on an initial rough, pre-CMP silicon wafer.

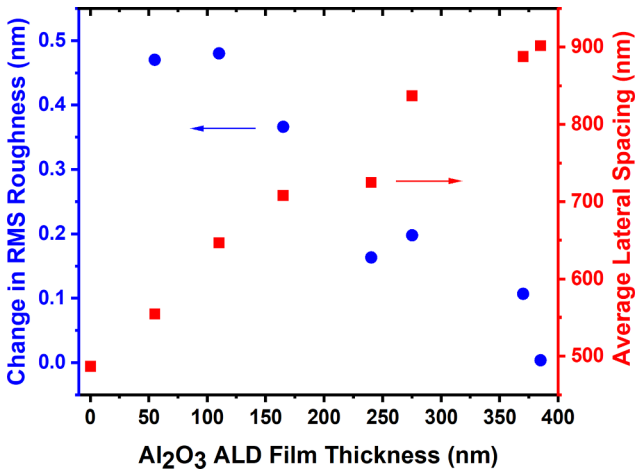

Fig. 7. Change in the RMS roughness for every 500 Al_2O_3 ALD cycles and average lateral spacing between the surface asperities versus Al_2O_3 ALD film thickness.

also shown for comparison. The decrease in the RMS roughness is 0.47 and 0.48 nm for the first 500 and second 500 Al_2O_3 ALD cycles, respectively. The change in the RMS roughness for the next subsequent sets of 500 Al_2O_3 ALD cycles then drops progressively for Al_2O_3 ALD film thicknesses $\geq$ 165 nm. In this regime, the average lateral spacing between surface asperities is $>$ 700 nm and much larger than the Al_2O_3 ALD film thickness. The ALD smoothing process becomes limited when the distance between the surface asperities is much larger than the ALD film thickness.

3.3. *Power spectral density analysis*

Power spectral density (PSD) analysis was performed to understand the lateral scale of the roughness that is affected by the Al_2O_3 ALD. PSD analysis is a spatial Fourier transform of the surface and characterizes the surface roughness in terms of spatial frequencies [26–28]. Fig. 8 shows the PSD analysis of the AFM spatial topography of the original rough silicon surface and this surface after various numbers of Al_2O_3 ALD cycles up to 4000 cycles. The spatial frequency on the x-axis represents the surface roughness at various lateral distances between the spatial features. A higher spatial frequency represents surface features

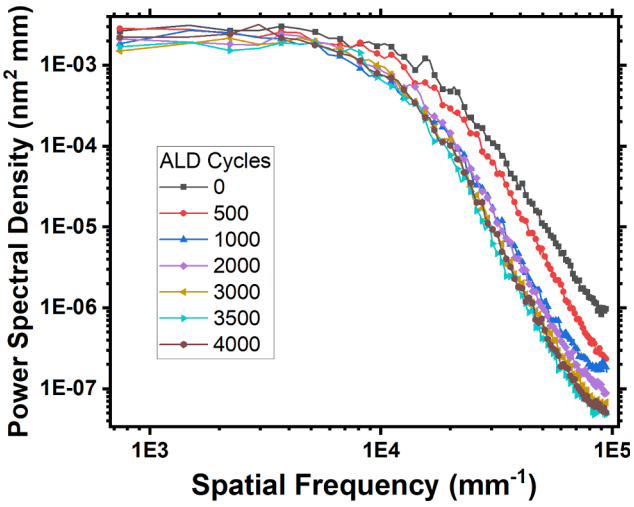

Fig. 8. PSD analysis of rough, pre-CMP silicon surfaces before and after various numbers of Al_2O_3 ALD cycles from AFM measurements.

that are closer together.

The PSD analysis given in Fig. 8 shows that the Al_2O_3 ALD causes the most change in the 10^5 to 10^4 mm^{-1} spatial range. This range equates to surface features that are on the order of 10s to 100s of nanometers apart. A change in this spatial range is expected given that the Al_2O_3 film thickness is on the order of 100s of nanometers. There are smaller changes as the spatial frequency decreases and distances between asperities are larger. The majority of the smoothing occurs during the first 1000 ALD cycles. Subsequently, the smoothing begins to level off after 1500 to 2000 ALD cycles that deposit Al_2O_3 film thicknesses of 165 to 240 nm, respectively. The smoothing at the largest spatial frequencies should reduce plasmon absorption from metal films deposited on these surfaces.

PSD analysis derived from WLI measurements can probe the surface smoothing at lower spatial frequencies. The PSD analysis of the WLI measurements in Fig. 9 indicates that the Al_2O_3 ALD film can also smooth micron scale roughness. There is a decrease in the PSD for spatial frequencies ranging from 30 mm^{-1} to 300 mm^{-1} or spatial distances ranging from 3.3 to 33 μm. At these lower spatial frequencies and larger spatial feature sizes, there is a progressive reduction in the PSD from 0 to 1000 to 3000 ALD cycles. The smoothing at lower spatial frequencies should help improve optical scattering from these surfaces.

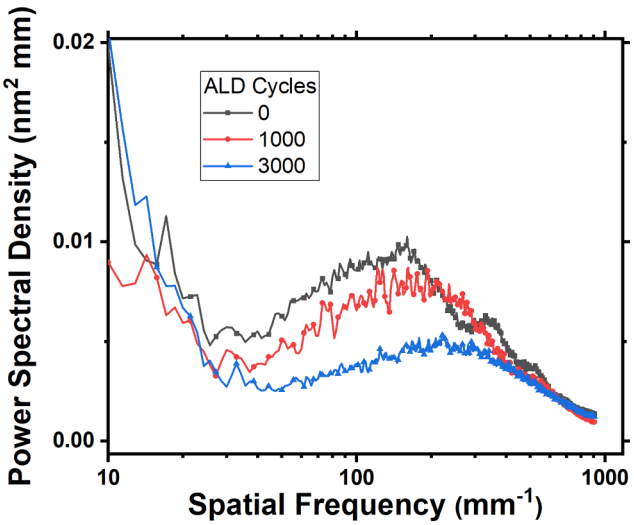

Fig. 9. PSD analysis of rough, pre-CMP silicon surfaces before and after various numbers of Al_2O_3 ALD cycles from WLI measurements.

A comparison between the PSD results shown in Figs. 8 and 9 indicates that the PSD reduction at the 10 μm scale is much less than the PSD reduction at the 10 nm scale. The PSD decrease after 1000 ALD cycles at the 10 nm scale (1E5 mm^{-1}) in Fig. 8 is about one order of magnitude. In comparison, the PSD decrease after 1000 ALD cycles at the 10 μm scale (100 mm^{-1}) in Fig. 9 is less than a factor of 2. This difference is anticipated because the thin ALD film thickness of ~ 100 nm should impact the nanometer scale lateral roughness more than the micron scale lateral roughness.

3.4. Specular reflectance measurements

Specular reflectance measurements were also performed on protected silver films with a thickness of 300 nm deposited using E-beam PVD on the original rough silicon surface and on the original rough silicon surface coated using various numbers of Al_2O_3 ALD cycles. These reflectance measurements can determine whether Al_2O_3 ALD smoothing can reduce optical scattering and surface absorption caused by surface roughness and improve optical performance. Fig. 10 displays the percent reflectance of the original, pre-CMP silicon substrate coated with a silver film. Specular reflectance measurements for the silicon substrate coated with a silver film after 1000, 2000, and 3000 Al_2O_3 ALD cycles are also displayed for comparison.

Fig. 10 shows that the specular reflected light from the silver film on the original rough silicon substrate decreases significantly for wavelengths shorter than 450 nm. These wavelengths are much longer than the sharp reflection minimum near 326 nm for silver mirrors [29]. The reflectance is only 25% at 370 nm. This low reflectivity is attributed primarily to surface absorption by surface plasmons enabled by surface roughness with feature sizes less than the light wavelength [22,23].

In comparison, Fig. 10 reveals that there is a progressive increase of reflectance for wavelengths between 350 and 600 nm versus number of Al_2O_3 ALD cycles. The largest reflectance gains are observed for the shorter wavelengths between 350 and 450 nm where the reflectance increase is as large as 35%. This wavelength region is also similar to the thickness of the deposited Al_2O_3 film of 370 nm after 3000 Al_2O_3 ALD cycles. These results suggest that Al_2O_3 ALD film thicknesses that smooth lateral surface roughness with feature sizes less than or similar to the light wavelength can have a pronounced effect on surface reflectance. This improved surface reflectance is attributed to less absorbance from surface plasmons.

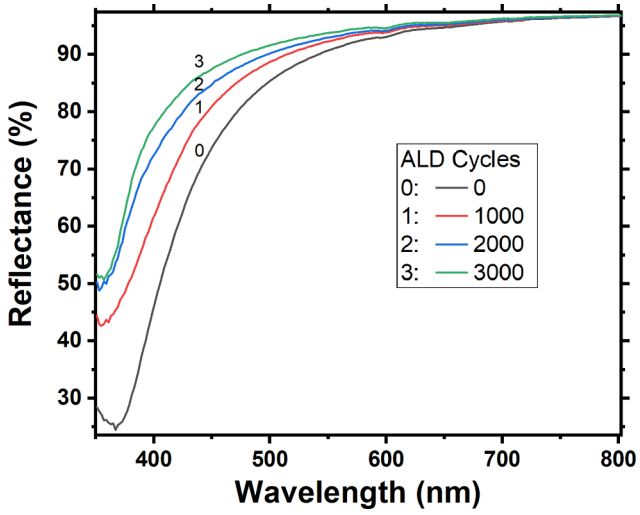

Fig. 10. Specular reflectance of silver films coated on the rough, pre-CMP silicon wafers and these substrates after 1000, 2000, and 3000 Al_2O_3 ALD cycles that deposit Al_2O_3 film thicknesses of 110, 240 and 370 nm, respectively.

3.5. Surface smoothing by thermal atomic layer etching

The lateral profile of the surface roughness is the most important consideration to determine the smoothing strategy. Two surfaces with the same RMS roughness could have very different lateral profiles. For example, the surface asperities could be tall, thin and spaced a large lateral distance apart. Alternatively, the surface asperities could be more rounded with comparable heights, widths and lateral spacings. Surface smoothing using ALD will be most effective for surface asperities that have small lateral spacings. The small gaps between the surface asperities will be easily "pinched off" by the ALD coating.

In addition to surface smoothing using ALD, thermal atomic layer etching (ALE) [30,31], may also help to reduce surface roughness. For example, there may be surfaces where the surface peaks are far apart but the width of the surface asperities is small. The large lateral spacing between these surface asperities would be difficult for ALD to "pinch-off". However, these surface peaks may be easy to erode using ALE. There are reports of both plasma and thermal ALE processes smoothing surface roughness [31–35]. There may also be some surfaces that would benefit from a hybrid ALD/ALE smoothing process. There are many avenues to explore concerning the use of ALD and ALE for smoothing surface roughness.

4. Conclusions

Al_2O_3 ALD has been demonstrated for smoothing surface roughness. For the pre-CMP silicon wafers, the average RMS roughness decreased from 3.3 nm to 1.5 nm and the average lateral spacing between the surface asperities increased from ≈490 nm to ≈890 nm after 3000 ALD cycles. The smoothing effect began to decrease when the thickness of the ALD film was greater than approximately one-half the original lateral separation distance between the surface asperities. ALD can smooth surface roughness until the average lateral distance between the spatial features is too large for the ALD film thickness to "pinch-off" the asperities.

PSD analysis showed that the ALD film thickness has the largest effect on spatial features that are 10s to 100s of nanometers apart. In addition, most smoothing occurred during the first 1000 Al_2O_3 ALD cycles. Surfaces coated with silver films showed a significant increase in reflectance at wavelengths below 450 nm. At these shorter wavelengths, the Al_2O_3 ALD film thicknesses are believed to smooth the surface roughness that enables light absorption by surface plasmons. Smoothing surface roughness with ALD should have important applications in many areas including optics.

CRediT authorship contribution statement

Tyler J. Myers: Formal analysis, Investigation, Resources, Data curation, Writing-original draft, Writing – review & editing, Visualization. **James A. Throckmorton:** Conceptualization, Methodology, Writing – review & editing, Supervision, Project administration. **Rebecca A. Borrelli:** Writing – review & editing. **Malcolm O'Sullivan:** Methodology, Formal analysis, Writing – review & editing. **Tukaram Hatwar:** Writing – review & editing. **Steven M. George:** Conceptualization, Methodology, Writing – review & editing, Visualization, Supervision, Project administration, Funding acquisition.

Declaration of Competing Interest

The authors declare that they have no known competing financial interests or personal relationships that could have appeared to influence the work reported in this paper.

Acknowledgements

This research was funded by Space & Airborne Systems at L3Harris. The authors thank Laurent Viravaux of Soitec for sending the rough, pre-CMP SOI silicon wafers for these surface smoothing studies.

References

[1] A. Sasaki, M. Ishino, M. Nishikino, An estimation of line width roughness of photoresists due to photon shot noise for extreme ultraviolet lithography using the percolation model, Jpn. J. Appl. Phys. 58 (5) (2019) 055002.
[2] G. Wang, Y. Wang, J.Z. Wang, L.J. Pan, L.W. Yu, Y.D. Zheng, Y. Shi, An Optimized FinFET Channel With Improved Line-Edge Roughness and Linewidth Roughness Using the Hydrogen Thermal Treatment Technology, IEEE Trans. Nanotechnol. 16 (2017) 1081–1087.
[3] S. Schröder, T. Feigl, A. Duparré, A. Tünnermann, EUV reflectance and scattering of Mo/Si multilayers on differently polished substrates, Opt. Express 15 (21) (2007) 13997.
[4] N.B. Zhong, X. Zhu, Q. Liao, Y.Z. Wang, R. Chen, Y.H. Sun, Effects of surface roughness on optical properties and sensitivity of fiber-optic evanescent wave sensors, Appl. Opt. 52 (2013) 3937–3945.
[5] F. Svahn, Å. Kassman-Rudolphi, E. Wallén, The influence of surface roughness on friction and wear of machine element coatings, Wear 254 (11) (2003) 1092–1098.
[6] A.G. Peressadko, N. Hosoda, B.N.J. Persson, Influence of surface roughness on adhesion between elastic bodies, Phys. Rev. Lett. 95 (12) (2005).
[7] C. Yang, U. Tartaglino, B.N.J. Persson, Influence of surface roughness on superhydrophobicity, Phys. Rev. Lett. 97 (11) (2006).
[8] C.B. Zarowin, Comparison of the smoothing and shaping of optics by plasma-assisted chemical etching and ion milling using the surface evolution theory, Appl. Opt. 32 (1993) 2984–2991.
[9] I. Ali, S.R. Roy, G. Shinn, Chemical-mechanical polishing of interlayer dielectric - A review, Solid State Technol. 37 (1994) 63.
[10] P.B. Zantye, A. Kumar, A.K. Sikder, Chemical mechanical planarization for microelectronics applications, Mater. Sci. Eng. R Rep. 45 (2004) 89–220.
[11] D. Golini, I. Kordonski, P. Dumas, and S. J. Hogan, Magetorheological finishing (MRF) in commerical precision optics manufacturing, Proc. SPIE 3782 Optical Manufacturing and Testing III, (1999) 80-91.
[12] D. Landolt, P.F. Chauvy, O. Zinger, Electrochemical micromachining, polishing and surface structuring of metals: fundamental aspects and new developments, Electrochim. Acta 48 (2003) 3185–3201.
[13] F. Frost, R. Fechner, B. Ziberi, J. Vollner, D. Flamm, A. Schindler, Large area smoothing of surfaces by ion bombardment: fundamentals and applications, J. Phys.: Condens. 21 (Matter 2009,), 224026.
[14] S.M. George, Atomic layer deposition: An overview, Chem. Rev. 110 (2010) 111–131.
[15] V. Miikkulainen, M. Leskela, M. Ritala, R.L. Puurunen, Crystallinity of inorganic films grown by atomic layer deposition: Overview and general trends, J. Appl. Phys. 113 (2013), 021301.
[16] E.R. Cleveland, P. Banerjee, I. Perez, S.B. Lee, G.W. Rubloff, Profile evolution for conformal atomic layer deposition over nanotopography, ACS Nano 4 (8) (2010) 4637–4644.
[17] J.W. Elam, Z.A. Sechrist, S.M. George, ZnO/Al_2O_3 nanolaminates fabricated by atomic layer deposition: growth and surface roughness measurements, Thin Solid Films 414 (1) (2002) 43–55.
[18] W.S. Lau, J. Zhang, X. Wan, J.K. Luo, Y. Xu, H. Wong, Surface smoothing effect of an amorphous thin film deposited by atomic layer deposition on a surface with nano-sized roughness, AIP Adv. 4 (2) (2014) 027120.
[19] F.B. Li, Y. Yang, Y.Q. Fan, W.H. Xing, Y. Wang, Modification of ceramic membranes for pore structure tailoring: The atomic layer deposition route, J. Membr. Sci. 397 (2012) 17–23.
[20] Z.A. Sechrist, F.H. Fabreguette, O. Heintz, T.M. Phung, D.C. Johnson, S.M. George, Optimization and structural characterization of W/Al_2O_3 nanolaminates grown using atomic layer deposition techniques, Chem. Mater. 17 (2005) 3475–3485.
[21] O. Stenzel, Optical Coatings: Material Aspects in Theory and Practice, Springer, 2014.
[22] S.-K. Kim, H.-S. Ee, W. Choi, S.-H. Kwon, J.-H. Kang, Y.-H. Kim, H. Kwon, H.-G. Park, Surface-plasmon-induced light absorption on a rough silver surface, Appl. Phys. Lett. 98 (1) (2011) 011109.
[23] J. Springer, A. Poruba, L. Mullerova, M. Vanecek, O. Kluth, B. Rech, Absorption loss at nanorough silver back reflector of thin-film silicon solar cells, J. Appl. Phys. 95 (2004) 1427–1429.
[24] J.W. Elam, M.D. Groner, S.M. George, Viscous flow reactor with quartz crystal microbalance for thin film growth by atomic layer deposition, Rev. Sci. Instrum. 73 (2002) 2981–2987.
[25] M.D. Groner, F.H. Fabreguette, J.W. Elam, S.M. George, Low-temperature Al_2O_3 atomic layer deposition, Chem. Mater. 16 (2004) 639–645.
[26] P. Dash, P. Mallick, H. Rath, A. Tripathi, J. Prakash, D.K. Avasthi, S. Mazumder, S. Varma, P.V. Satyam, N.C. Mishra, Surface roughness and power spectral density study of SHI irradiated ultra-thin gold films, Appl. Surf. Sci. 256 (2009) 558–561.
[27] Y. Gong, S.T. Misture, P. Gao, N.P. Mellott, Surface roughness measurements using power spectrum density analysis with enhanced spatial correlation length, J. Phys. Chem. C 120 (39) (2016) 22358–22364.
[28] J.M. Elson, J.M. Bennett, Calculation of the power spectral density from surface profile data, Appl. Opt. 34 (1995) 201–208.
[29] R.E. Hummel, Reflectivity of silver-based and aluminum-based alloys for solar reflectors, Sol. Energy 27 (1981) 449–455.
[30] S.M. George, Mechanisms of thermal atomic layer etching, Acc. Chem. Res. 53 (2020) 1151–1160.

[31] Y. Lee, S.M. George, Atomic layer etching of Al_2O_3 using sequential, self-limiting thermal reactions with $Sn(acac)_2$ and hydrogen fluoride, ACS Nano 9 (2) (2015) 2061–2070.
[32] A.I. Abdulagatov, S.M. George, Thermal atomic layer etching of silicon nitride using an oxidation and "conversion etch" mechanism, J. Vac. Sci. Technol. A 38 (2) (2020) 022607.
[33] K.J. Kanarik, S. Tan, R.A. Gottscho, Atomic layer etching: Rethinking the art of etch, J. Phys. Chem. Lett. 9 (16) (2018) 4814–4821.
[34] Y. Lee, J.W. DuMont, S.M. George, Atomic layer etching of HfO_2 using sequential, self-limiting thermal reactions with $Sn(acac)_2$ and HF, ECS J. Solid State Sci. Technol. 4 (6) (2015) N5013–N5022.
[35] D.R. Zywotko, J. Faguet, S.M. George, Rapid atomic layer etching of Al_2O_3 using sequential exposures of hydrogen fluoride and trimethylaluminum with no purging, J. Vac. Sci. Technol. A 36 (6) (2018) 061508.